Available online at www.sciencedirect.com

ScienceDirect

MATTER AND RADIATION AT EXTREMES

Matter and Radiation at Extremes 2 (2017) 256–262

www.journals.elsevier.com/matter-and-radiation-at-extremes

Research Article

Laser radiation pressure proton acceleration in gaseous target

V.K. Tripathi [a], Tung-Chang Liu [b,*], Xi Shao [b]

[a] *Physics Department, Indian Institute of Technology Delhi, New Delhi 110016, India*
[b] *Department of Physics, University of Maryland, College Park, MD 20742, USA*

Received 2 March 2017; revised 19 June 2017; accepted 3 July 2017
Available online 12 August 2017

Abstract

An analytical model for hole boring proton acceleration by a circularly-polarized CO_2 laser pulse in a gas jet is developed. The plasma density profile near the density peak is taken to be rectangular, with inner region thickness l around a laser wavelength and density 10% above the critical, while the outside density is 10% below the critical. On the rear side, plasma density falls off rapidly to a small value. The laser suffers strong reflection from the central region and, at normalized amplitude $a_0 \geq 1$, creates a double layer. The space charge field of the double layer, moving with velocity $v_f\hat{z}$, reflects up-stream protons to $2v_f$ velocity, incurring momentum loss at a rate comparable to radiation pressure. Reflection occurs for $v_f \leq \omega_p\sqrt{z_f lm/m_p}$, where m and m_p are the electron and proton masses, z_f is the distance traveled by the compressed electron layer and ω_p is the plasma frequency. For Gaussian temporal profile of the laser and parabolic density profile of the upstream plasma, the proton energy distribution is narrowly peaked.

PACS Codes: 41.75.Jv; 52.27.Ny; 52.38.Kd

Keywords: Laser-driven acceleration; Radiation pressure proton acceleration; Relativistic plasmas

1. Introduction

Laser-driven proton acceleration is an active field of research due to its potential applications, including proton therapy of tumor. The prominent schemes of acceleration are target normal sheath acceleration [1–4], hole boring [5,6], radiation pressure acceleration [7–13] and shock acceleration [13]. While many experiments employ thin foil targets irradiated by 1.06 μm or 0.8 μm laser, some experiments [14–16] have been conducted on gas jet targets irradiated by 10.6 μm CO_2 laser micropulses.

Palmer et al. [15] have reported the generation of 1 MeV proton beam with 4% energy spread using 6 ps circularly-polarized CO_2 laser pulses of intensity $I \leq 10^{16}$ W/cm^2 (normalized amplitude of $a_0 \leq 0.5$) on a hydrogen jet with triangular density profile of width $L_n = 825$ μm and density peak of 10 times the critical value, i.e., $n_{0max} = 10n_{cr}$. The results are interpreted as hole boring acceleration where radiation pressure driven plasma front pushes the upstream protons to twice the shock front velocity.

Haberberger et al. [16] have conducted experiments with 3 ps linearly-polarized CO_2 laser micropulses of intensity $I \leq 6.6 \times 10^{16}$ W/cm^2 ($a_0 \approx 1.5 - 2.5$) impinged on a hydrogen jet of density peak 3 to 5 times n_{cr}. They observe steepened plasma density profile and generation of 22 MeV protons with 1% energy spread. PIC simulations reveal formation of an electrostatic shock that reflects upstream protons with energy comparable to the one observed, but with much larger energy spread. It is claimed that the shock is not driven by radiation pressure because that would lead to much lower energies.

These experiments have brought into focus two scenarios of hole boring acceleration. In the first case, a

* Corresponding author.
E-mail address: tcliu@umd.edu (T.-C. Liu).
Peer review under responsibility of Science and Technology Information Center, China Academy of Engineering Physics.

http://dx.doi.org/10.1016/j.mre.2017.07.001

circularly-polarized laser of intensity I impinged on an overdense plasma half space of density n pushes the plasma ahead of it as a piston. The piston acquires a velocity v_f at which the rate of momentum imparted to the upstream plasma equals the radiation pressure. $2I/c = 2nm_p v_f^2$, giving ion energy $\varepsilon_p = 2m_p v_f^2 = 2I/nc$; here m_p is the ion mass and $c$is the speed of light in vacuum. Palmer et al. [15] observe this sort of dependence of proton energy on I/n. Robinson et al. [17] have generalized the problem to relativistic speeds. Macchi and Benedetti [18] provide a physical picture of moving layer as an electron ion double layer, created by the laser ponderomotive force. The moving double layer accelerates upstream ions. These theories, however, consider plasma of uniform density.

In the second case, a linearly-polarized laser pulse exerts a second harmonic ponderomotive force on electrons and heats them locally to temperature $T_e = mc^2(\gamma - 1)$, where $\gamma = (1 + a_0^2/2)^{1/2}$, m is the electron rest mass. This creates a shock front. As the shock propagates with supersonic speed, it reflects the upstream ions at twice its speed imparting them large energy as reported by Haberberger et al. Levy et al. [19] have looked into the hole boring problem under the combined effects of piston action and plasma heating.

Ji et al. [20] have put forth the scheme of radiation-pressure-driven dragging-field proton acceleration. They consider an overdense hydrogen plasma foil in a very-low-density upstream plasma. The laser ponderomotive force pushes the foil electrons, leaving behind an extended ion space charge. As this structure, under radiation pressure, moves ahead, its space charge field (dragging field) reflects the upstream protons imparting them high energy. For $a_0 \approx 200$, the scheme predicts energies in hundreds of GeV but with large energy spread. The analytical treatment ignores the momentum loss of the moving structure to upstream protons. Yu et al. [21] and Zheng et al. [22] also consider the ultra-relativistic laser irradiance ($a_0 = 250$) and a foil thickness smaller than the one required for the formation of quasi-static double layer. The upstream plasma has a low charge-to-mass ratio ($Z/A = 1/3$) and a very low density. Their 1D PIC simulations reveal snow plow accumulation of upstream plasma electrons at the radiation-pressure-compressed layer of foil electrons. The heavier upstream ions, however, are run over by the moving proton-electron double layer. The space charge field seen by the protons gets strengthened and the protons may be accelerated to hundreds of GeV energy in a distance of 1 cm, if the double layer preserves its stability in two dimensions.

In this paper, we present a scenario of dragging field acceleration of protons in a hydrogen jet irradiated by a circularly-polarized CO_2 laser pulse. For a plasma slab of thickness of the order of laser wavelength and density 10% above critical, with the outside plasma density 10% below critical, we note that the laser exerts a large radiation pressure force $\sim 1.9I/c$ on slab electrons and creates an ion-electron double layer. As the double layer is accelerated, it incurs momentum loss to upstream protons. We choose a density profile with the flat central peak slightly above the relativistic critical density and the outside density below critical. A couple of wavelengths away the upstream plasma density drops down to low values. As the double layer propagates through the under-dense hydrogen plasma of density $n_u(z)$ with velocity $v_f\hat{z}$, the velocity of plasma ions measured in the frame moving with the front is $-v_f\hat{z}$. They suffer reflection due to the space charge field of the moving front with velocity $v_f\hat{z}$ with respect to the front. The double layer suffers a net retardation force due to these protons.

In Sec. 2 we study laser reflection from a near-critical density plasma slab placed in a slightly underdense plasma and then consider a gas jet with parabolic density profile and deduce the condition for profile steepening and double layer formation. In Sec. 3 we study the velocity evolution of the double layer pushed by the radiation pressure and losing momentum to the reflected upstream protons. In Sec. 4 we discuss the results.

2. The model problem

2.1. Laser reflection from a near-critical density plasma slab

Consider a circularly-polarized-CO_2-laser-irradiated hydrogen gas jet with a parabolic density profile, having a peak density slightly more than the relativistic critical density. In order to appreciate plasma density profile steepening and formation of a double layer near the density peak, we begin with the linear problem of reflection of a laser beam of frequency ω normally incident on a rectangular plasma density profile (Fig. 1), expressed in terms of plasma frequency as

$$\omega_p^2 = \begin{cases} \omega_{p1}^2 & \text{for } |z| > l, \\ \omega_{p2}^2 & \text{for } |z| < l. \end{cases} \tag{1}$$

The intensity transmission coefficient of the slab is

$$T = \frac{16\alpha^2\eta^2}{\left|(\alpha + i\eta)^2 e^{-\omega\alpha l/c} - (\alpha - i\eta)^2 e^{\omega\alpha l/c}\right|^2}, \tag{2}$$

where $\eta = (1 - \omega_{p1}^2/\omega^2)^{1/2}$, $\alpha = (\omega_{p2}^2/\omega^2 - 1)^{1/2}$ and c is the speed of light in vacuum. In a special case of $\omega_{p2}^2/\omega^2 - 1 = 1 - \omega_{p1}^2/\omega^2$ (i.e., density in the slab is above the critical density by the same amount as it is below critical density outside), $\alpha = \eta$, the above expression reduces to

$$T = \frac{1}{\cosh^2(\omega\alpha l/c)}. \tag{3}$$

For $l \approx 2\pi c/\omega = \lambda_L$ (laser wavelength), a gentle density step, corresponding to $\omega_{p2}^2/\omega^2 = 1.04$ and $\omega_{p1}^2/\omega^2 = 0.96$ (i.e., with 8% density change), gives $T \approx 0.4$, a substantially reduced transmittivity. For $\omega_{p2}^2/\omega_L^2 = 1.1$ and $\omega_{p1}^2/\omega_L^2 = 0.9$ (20% density change), $T \approx 0.06$, i.e., the transmittivity is severely reduced. The laser of intensity I exerts a radiation force

$$F_p = \frac{2I}{c}(1 - T) \tag{4}$$

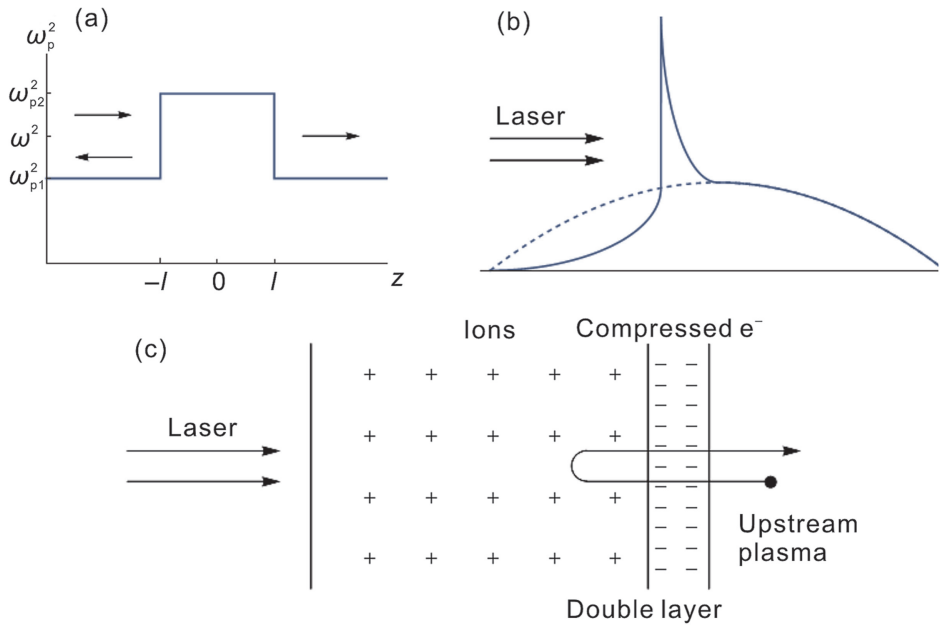

Fig. 1. (a) A rectangular plasma density profile irradiated by CO_2 laser from the left. (b) The parabolic plasma density profile of a gas jet with an elevated peak created by radiation pressure. The peak turns into a moving double layer. (c) In the moving frame of the double layer, upstream protons enter the layer with velocity $-v_f\hat{z}$ and leave with $v_f\hat{z}$.

on the plasma slab, which is close to the radiation pressure a plasma slab placed in vacuum would experience.

2.2. Parabolic density profile: laser induced steepening

Now consider a parabolic density profile, encountered in gas jet targets,

$$\omega_p^2 = \begin{cases} \omega_{p0}^2\left(1 - z^2/L_n^2\right) & \text{for } |z| < L_n, \\ 0 & \text{otherwise.} \end{cases} \tag{5}$$

A laser pulse impinges on it from the left with electric field

$$\boldsymbol{E} = A(\hat{\boldsymbol{x}} + \mathrm{i}\hat{\boldsymbol{y}})\exp[-\mathrm{i}\omega(t - z/c)],$$
$$A^2 = A_0^2 \exp\left[-\left(\frac{t - z/c}{\tau_L}\right)^2\right]. \tag{6}$$

The low amplitude portion of the pulse reflects from

$$z = -z_0 = -\sqrt{1 - \omega^2/\omega_{p0}^2}L_n, \tag{7}$$

whereas the high amplitude portion of the pulse reflects from

$$z = -z_m = -\sqrt{1 - \omega^2\gamma_0/\omega_{p0}^2}L_n, \tag{8}$$

where $\gamma_0 = (1 + a_0^2)^{1/2}$, $a_0 = (eA_0/m\gamma_0 c)G$, $A_0 = (\mu_0 c I_0)^{1/2}$, μ_0 is the free space permeability, n_{cr} is the critical density and $-e$ and m are the electronic charge and rest mass. γ_0 contains a factor G that accounts for dielectric swelling (increase in laser amplitude as it approaches higher and higher density). For $\omega_{p0}^2/\gamma_0\omega^2 \approx 1$, the distance between the two reflection points is about $z_0 \approx L_n$. The pulse covers this distance in time τ_L. Thus the velocity of critical layer propagation is $v_c \approx L_n/\tau_L$. Let us compare this with the speed with which plasma is pushed by the radiation pressure. The acceleration of the plasma of width l (having ln_0m_p mass per unit area) is

$$g = \frac{2I_0(1-T)}{cl\,n_0m_p} = a_0^2\frac{m}{m_p}\frac{c^2\omega^2}{\omega_p^2 l}(1-T). \tag{9}$$

Time taken by the plasma to cover a distance of nearly z_0 is $\tau_i = (2z_0/g)^{1/2}$. This time should be smaller or equal to pulse duration τ_L, i.e.,

$$a_0^2 > 2\frac{m_p}{m}\frac{lL_n}{c^2\tau_L^2}. \tag{10}$$

For $l \approx 10$ μm, this condition amounts to $L_n \leq 2.2\tau_L^2 a_0^2$, where τ_L is in picoseconds and L_n is in micrometers. In Fig. 2 we have plotted the density scale length versus normalized laser intensity boundary below which profile steepening would occur. For $L_n \approx 40$ μm and $\tau_L = 3$ ps, steepening would occur for $a_0^2 > 2$. In case of succession of pulses one may achieve it at smaller values of normalized laser amplitude. Haberberger et al. [16] observed such a profile with linearly-polarized CO_2 laser of $a_0 \approx 2.5$. One should observe it with circular polarization too. Once a narrow overdense plasma peak is created by the train of pulses, a subsequent pulse sees it as an overdense plasma foil, and polarizes it, creating a moving double-layer.

3. Radiation-pressure-assisted hole boring acceleration

The radiation pressure force on the double layer of areal mass density n_0m_pl, in the non-relativistic limit, is $2I/c$ per unit area. The momentum loss rate to the upstream protons of mass m_p is $2n_um_pv_f^2$. Hence, the equation of motion governing velocity v_f of the double layer is

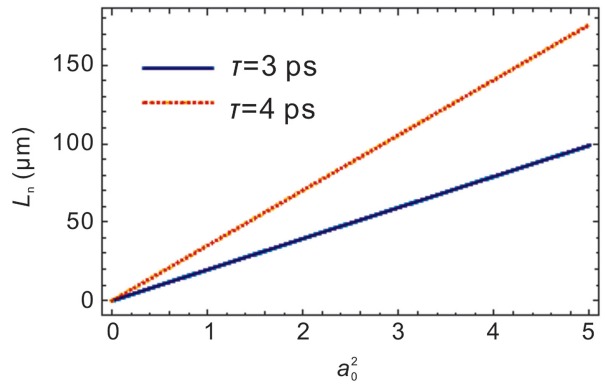

Fig. 2. Boundary line in density-scale-length-normalized intensity parameter space. Below the line ponderomotive-force-led profile steepening occurs.

$$n_0 m_p l \frac{dv_f}{dt} = \frac{2I}{c} - 2n_u m_p v_f^2. \tag{11}$$

One may mention that the reflection of upstream protons from the double layer occurs due to the space charge field in the double layer, primarily in the ion region; in the compressed electron layer the field falls from $n_0 el/\varepsilon_0$ to zero in a shorter distance. Initially the field in the ion layer is $E_s = n_0 ez/\varepsilon_0$. However, with time the ion layer spreads. At time t it extends from $z = 0$ to $z = z_f = n_0 e^2 l t^2/2\varepsilon_0 m_p$ (in the non-relativistic limit) with ion density and space charge field

$$n_i = \frac{n_0}{1 + z_f/l},\ E_s = \frac{n_0 ez}{(1 + z_f/l)\varepsilon_0}. \tag{12}$$

The potential difference across the layer is

$$\varphi_s = \frac{n_0 e z_f^2}{2\varepsilon_0 (1 + z_f/l)}. \tag{13}$$

The upstream proton will suffer reflection from the layer when $e\varphi_s > m_p v_f^2/2$, i.e.,

$$v_f \le \sqrt{\frac{n_0 e^2}{m_p \varepsilon_0} \frac{z_f^2}{1 + z_f/l}} \approx \omega_p \sqrt{z_f l} \sqrt{\frac{m}{m_p}}\ , \tag{14}$$

and the maximum proton energy gain in the laboratory frame is

$$\varepsilon_{pm} = 2m_p v_f^2 = 2m\omega_p^2 \sqrt{z_f l}. \tag{15}$$

Writing $dv_f/dt = v_f dv_f/dz$ one may write Eq. (11) as

$$\frac{d}{dz} v_f^2 + \frac{4n_u(z)}{n_0 l} v_f^2 = 2\frac{a_0^2 c^2}{l} \frac{n_{cr}}{n_0} \frac{m}{m_p}. \tag{16}$$

In the case when laser amplitude is constant in time, this equation integrates to give

$$v_f^2 = \left[v_{f0}^2 + 2\frac{a_0^2 c^2}{l} \frac{n_{cr}}{n_0} \frac{m}{m_p} \int_0^z e^{h(z)} dz \right] e^{-h(z)},$$
$$h(z) = \frac{1}{n_0 l} \int_0^z n_u(z) dz, \tag{17}$$

where $v_f = v_{f0}$ at $z = 0$.

For a constant density upstream Eq. (17) takes the form

$$v_f^2 = v_{f0}^2 + \frac{a_0^2 c^2}{2} \frac{n_{cr}}{n_u} \frac{m}{m_p} \left(1 - e^{-\frac{4n_u z}{n_0 l}} \right). \tag{18}$$

One may notice the enhancement in velocity due to reduction in upstream plasma density n_u. For $n_u/n_{cr} = 0.1$, $a_0 = 2.5$, $v_{f0} = 0$, one may achieve $v_f/c = 0.13$, giving proton energy $\varepsilon_p = 2m_p v_p^2 \approx 30$ MeV.

In the case of linear density profile upstream, $n_u = n_0'(1 - z/L_n)$ for $z < L_n$, one obtains

$$v_f^2 = \left\{ v_{f0}^2 \exp\left(\frac{l_n^2}{l_0^2} \right) + 2a_0^2 c^2 \frac{n_{cr}}{n_0} \frac{m}{m_p} \left[\mathrm{erf}\left(\frac{l_n}{l_0} \right) - \mathrm{erf}\left(\frac{l_n - z}{l_0} \right) \right] \right.$$
$$\left. \times \right\} \exp\left[\left(\frac{z - l_n}{l_0} \right)^2 \right], \tag{19}$$

where $l_0 = \sqrt{2n_0 l_n l/n_0'}$. As $z \to L_n$ and if one takes $2l_n/l_0 \gg 1$ and $v_{f0} = 0$, one obtains

$$\frac{v_f^2}{c^2} = a_0^2 \frac{n_{cr}}{n_0} \frac{m}{m_p} \sqrt{\frac{2n_0 l_n \pi}{n'_0 l}}. \tag{20}$$

For $a_0 = 2.5$, $n_{cr}/n_0 = 1/3$, $n'_0/n_0 = 0.1$, $m_p/m = 1836$ and $l_n/l = 40$, one obtains $v_f^2/c^2 = 0.03$ and proton energy $\varepsilon_p = 2m_p v_f^2 = 60$ MeV.

For a parabolic density profile, $n_u(z) = n_{u0}(1 - z^2/L_n^2)$,

$$h(z) = \frac{4n_{u0}}{n_0 l} z \left(1 - \frac{z^2}{3L_n^2} \right) \tag{21}$$

and Eq. (17), for $z \le 0.7L_n$, simplifies to

$$v_f^2 = v_{f0}^2 + \frac{a_0^2 c^2 m}{2m_p} \frac{n_{cr}}{n_{u0}} \left[1 - \exp\left(-4\frac{n_{u0}}{n_0} \frac{z}{l} \right) \right]. \tag{22}$$

In Fig. 3 we have plotted v_f/c as a function of n_{u0}/n_{cr} for $z/l = 25$ and $a_0^2 = 2.5$. The foil velocity, hence reflected proton energy, decreases with increasing n_{u0}/n_{cr} as momentum loss rate by the moving layer increases. For upstream density 1% of the critical density, the proton velocity turns out to be $0.4c$; whereas for upstream density 10% of the critical density, the proton velocity is $0.16c$.

3.1. Relativistic case

In case the double layer acquires relativistic velocity, Eq. (16) modifies to

$$\frac{d}{dz} v_f^2 + \frac{4n_u(z)}{\gamma_f n_0 l} v_f^2 = 2\frac{a_0^2 c^2}{l} \frac{n_{cr}}{n_0} \frac{m}{m_p \gamma_f^3} \frac{1 - v_f/c}{1 + v_f/c}, \tag{23}$$

where $\gamma_f = (1 - v_f^2/c^2)^{-1/2}$ and we have used $d/dt = v_f d/dz$, $d(\gamma_f v_f)/dz = \gamma_f^3 dv_f/dz$. This equation differs from Ji et al.'s as they have neglected the second term on the left hand side. Equation (21) can be solved numerically for suitable profiles of $n_u(z)$. It can be written as

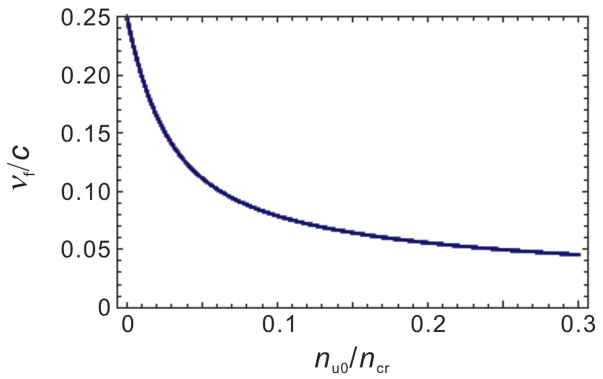

Fig. 3. Normalized velocity of the double layer as a function of n_{u0}/n_{cr} for parabolic density profile of upstream plasma for $z/l = 25$ and $a_0^2 = 2.5$.

$$\frac{\mathrm{d}v_\mathrm{f}}{\mathrm{d}t} = 2\frac{a_0^2c^2}{\gamma_\mathrm{f}^3 l}\frac{n_\mathrm{cr}}{n_0}\frac{m}{m_\mathrm{p}}\frac{1-v_\mathrm{f}/c}{1+v_\mathrm{f}/c} - \frac{n_{u0}}{n_0 l}\frac{v_\mathrm{f}^2}{\gamma_\mathrm{f}}\left(1-\frac{z^2}{L_\mathrm{n}^2}\right) \tag{24}$$

and solved in conjunction with

$$\frac{\mathrm{d}z}{\mathrm{d}t} = v_\mathrm{f},$$
$$a_0^2 = a_{00}^2 \exp\left[-\frac{1}{\tau_\mathrm{L}^2}\left(t-\frac{z}{c}\right)^2\right]. \tag{25}$$

The energy of double layer reflected protons is

$$\varepsilon_\mathrm{p} = m_\mathrm{p}c^2\left\{\left[1+\frac{4v_\mathrm{f}^2/c^2}{\left(1-v_\mathrm{f}^2/c^2\right)^2}\right]^{\frac{1}{2}} - 1\right\} = 2m_\mathrm{p}v_\mathrm{f}^2\gamma_\mathrm{f}^2. \tag{26}$$

3.2. Proton energy distribution function

We may deduce the proton energy distribution function as follows. The number of upstream protons reflected between z and $z + \mathrm{d}z$, per unit area, is

$$\mathrm{d}N = n_\mathrm{u}\mathrm{d}z. \tag{27}$$

These protons have energy in the range between ε_p and $\varepsilon_\mathrm{p} + \mathrm{d}\varepsilon_\mathrm{p}$, where [from Eq. (26)]

$$\mathrm{d}\varepsilon_\mathrm{p} = 2m_\mathrm{p}v_\mathrm{f}\gamma_\mathrm{f}^4\mathrm{d}v_\mathrm{f}. \tag{28}$$

Using this we may write

$$\mathrm{d}N = f\mathrm{d}\varepsilon_\mathrm{p}, \tag{29}$$

$$f = \frac{n_{u0}\left(1-z^2/L_\mathrm{n}^2\right)}{2m_\mathrm{p}v_\mathrm{f}\gamma_\mathrm{f}^4\frac{\mathrm{d}v_\mathrm{f}}{\mathrm{d}z}}. \tag{30}$$

We have solved Eqs. (24)–(30) numerically for the following parameters: $l\,n_0/n_\mathrm{cr} = a_0\lambda_\mathrm{L}/2\pi$, $\omega_\mathrm{L}\tau_\mathrm{L}/2\pi = 30$, $a_0 = 5$, $n_{u0}/n_\mathrm{cr} = 0.2$, 0.4 and $\omega_\mathrm{L}L_\mathrm{n}/2\pi c = 10$. In Fig. 4(a) we have plotted the normalized velocity of the double layer as a function of distance normalized to laser wavelength (v_f/c versus z/λ_L) for $n_{u0}/n_\mathrm{cr} = 0.2$. The velocity rises linearly initially and then attains almost a plateau when the radiation pressure nearly balances the momentum transfer rate to upstream protons. Beyond this point the velocity rises mildly in the tail of the laser pulse. Fig. 4(b) shows the normalized proton distribution function $F(\varepsilon_\mathrm{p}) = f2m_\mathrm{p}c^2/n_{u0}\lambda_\mathrm{L}$ as a function of energy in units of $2mc^2$, i.e., in MeV. The distribution function is narrowly peaked at $\varepsilon_\mathrm{p} \approx 150$ MeV. Fig. 5(a) and (b) show similar plots for $n_{u0}/n_\mathrm{cr} = 0.4$. The foil velocity rises with z as the momentum loss rate to reflected ions decreases due to their decreasing number. However, with a Gaussian pulse of lower intensity, the radiation pressure term in the tail of the pulse decreases with time and acquires values lower than the momentum loss term, hence the velocity of the double layer mildly decreases. The energy distribution function is more sharply peaked, while the energy ε_pm at which the peak occurs, decreases. Fig. 6 shows the plots for $n_{u0}/n_\mathrm{cr} = 0.2$, 0.4, 0.6 and $a_0 = 2.5$. The proton energy distribution is sharply peaked in all the three cases. However, the shoulders in energy distribution in Figs. 4 and 5 are symmetric, while in Fig. 6 these are asymmetric with an abrupt drop at the high energy side. The energy scaling with a_0 appears a bit faster than a_0^2. This seems to be due to the nonlinear nature of momentum loss rate to upstream ions. The optimum proton energy ε_pm decreases with the density of the upstream plasma.

4. Discussion

Radiation-pressure-driven hole boring proton acceleration, using circularly polarized laser, is similar to the dragging field

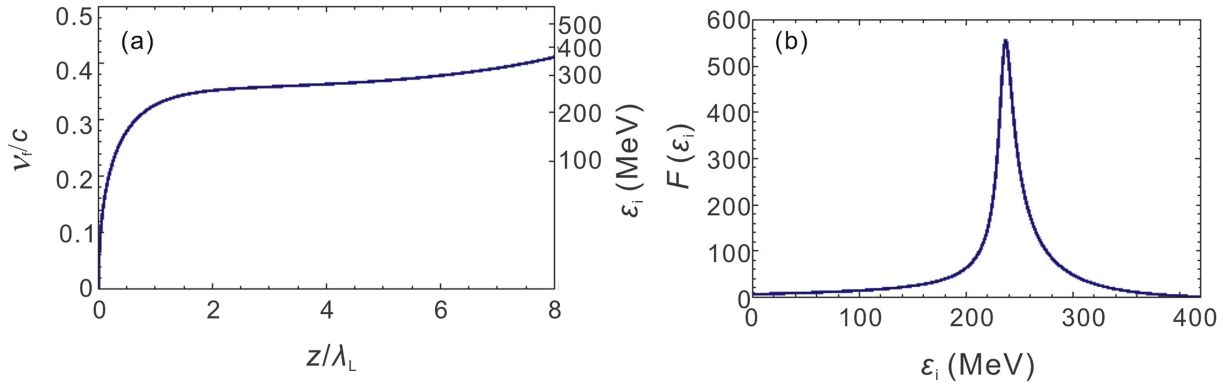

Fig. 4. Normalized velocity of the moving double layer (irradiated by a Gaussian laser pulse) through a plasma with parabolic density profile. The parameters are: $a_0 = 5.0$, $\omega_\mathrm{L}\tau_\mathrm{L}/2\pi = 30$ and $n_{u0}/n_\mathrm{cr} = 0.2$.

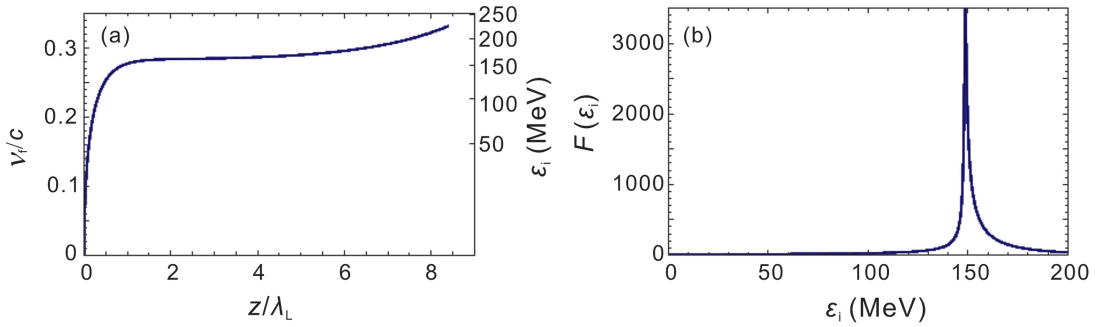

Fig. 5. Normalized velocity of the moving double layer (irradiated by a Gaussian laser pulse) through a plasma with parabolic density profile. The parameters are: $a_0 = 5.0$, $\omega_L\tau_L/2\pi = 30$ and $n_{u0}/n_{cr} = 0.4$.

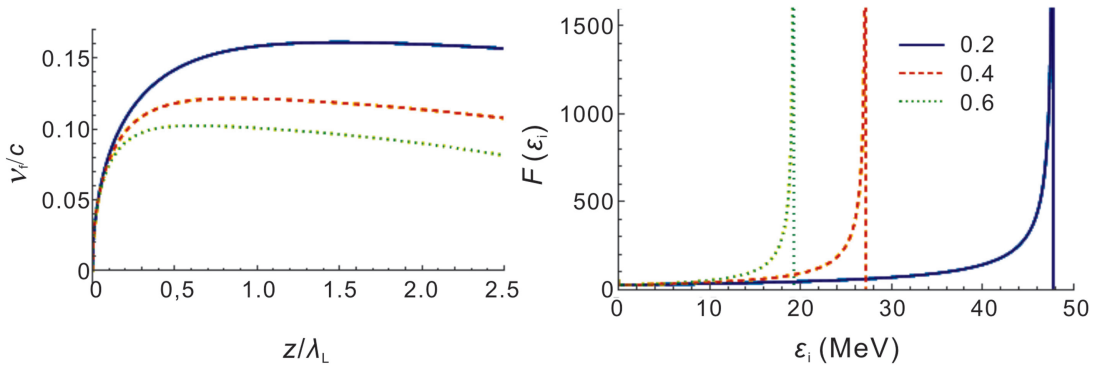

Fig. 6. Normalized velocity of the moving double layer (irradiated by a Gaussian laser pulse) through a plasma with parabolic density profile. The parameters are: $a_0 = 2.5$, $n_{u0}/n_{cr} = 0.2, 0.4, 0.6$ and $\omega_L\tau_L/2\pi = 30$.

ion acceleration of Ji et al. The crucial requirement is the formation of an overdense plasma double layer. It can be achieved by choosing a gas jet plasma of density close to the relativistic critical density and relying on the ponderomotive-induced steepening of the density profile to form a moving double layer. Ji et al. considered an ultrathin foil of overdense plasma while the upstream plasma was of very low density and the normalized laser amplitude was $a_0 \gg 1$. We explored the plasma near-critical density, considered a_0 around 1 or 2 and included momentum loss of the double layer to reflected upstream protons.

The combination of temporal Gaussian intensity profile of the laser and parabolic density profile of the upstream underdense plasma appears to be unique to ensure a stable double-layer velocity, which leads to a quasi-monoenergetic proton beam. The optimum energy ε_m at which the upstream proton energy distribution has a sharp peak, decreases with the increase in upstream plasma density. However, the reflection of upstream protons occurs as long as the double-layer velocity $v_f \leq \omega_p\sqrt{z_f lm/m_p}$. This condition limits the upstream proton energy to few-hundred-MeV range. The present treatment is applicable as long as the total number of protons reflected is significantly lower than the total number of protons in the double layer.

The treatment ignores shock formation, as for a circularly-polarized laser second harmonic ponderomotive force vanishes and electrons are not heated enough to give rise to a shock. For a shock to develop the electron pressure in the laser-compressed plasma must be comparable to the laser radiation pressure in order for the shock front to propagate away from the laser reflection region. Else we have hole-boring. With circular polarization one can also get density profile steepening and the dragging field of ensued double layer could as effectively reflect the upstream protons as the shock in the case of linear polarization. Palmer et al. employed larger density scale length hence their upstream plasma density is large. As a result they get smaller energies of reflected protons. Their laser intensity is also less than that of Haberberger et al. With proper structuring of density profile and laser temporal profile one may get quasi-monoenergetic protons of several tens of MeV with circularly-polarized CO_2 laser of intensity 10^{17} W/cm^2.

Recently Passoni et al. [23] have come up with nano-structured double layer targets, comprising carbon foam layer of density 7 mg/cm^3 on 0.75 μm thick aluminum foil. On irradiating it with 1 μm laser of $a_0 = 5$ they attained a plasma density near the critical density and obtained ion energies of the order of 30 MeV via TNSA. However, it raises the possibility of employing solid foils to create near-critical density plasma for RPA-hole boring at 1 μm laser wavelength.

The semi-analytical approach adopted here for the creation of double layer brings out the physics of the process and may act as a bench mark for state of the art PIC simulations. Sharpened density profiles have been reported for linear polarization.

References

[1] L. Robson, P.T. Simpson, R.J. Clarke, K.W.D. Ledingham, F. Lindau, et al., Scaling of proton acceleration driven by petawatt-laser−plasma interactions, Nat. Phys. 3 (2007) 58−62, http://dx.doi.org/10.1038/nphys476.

[2] J. Fuchs, P. Antici, E. d'Humières, E. Lefebvre, M. Borghesi, et al., Laser-driven proton scaling laws and new paths towards energy increase, Nat. Phys. 2 (2006) 48−54, http://dx.doi.org/10.1038/nphys199.

[3] A. Pukhov, Three-dimensional simulations of ion acceleration from a foil irradiated by a short-pulse laser, Phys. Rev. Lett. 86 (2001) 3562−3565, http://dx.doi.org/10.1103/PhysRevLett.86.3562.

[4] B.M. Hegelich, B.J. Albright, J. Cobble, K. Flippo, S. Letzring, et al., Laser acceleration of quasi-monoenergetic MeV ion beams, Nature 439 (2006) 441−444, http://dx.doi.org/10.1038/nature04400.

[5] M.S. Wei, S.P.D. Mangles, Z. Najmudin, B. Walton, A. Gopal, et al., Ion acceleration by collisionless shocks in high-intensity-laser-underdense-plasma interaction, Phys. Rev. Lett. 93 (2004) 155003, http://dx.doi.org/10.1103/PhysRevLett.93.155003.

[6] F. Fiuza, A. Stockem, E. Boella, R.A. Fonseca, L.O. Silva, et al., Ion acceleration from laser-driven electrostatic shocks, Phys. Plasmas 20 (2013) 056304, http://dx.doi.org/10.1063/1.4801526.

[7] X.Q. Yan, C. Lin, Z.M. Sheng, Z.Y. Guo, B.C. Liu, et al., Generating high-current monoenergetic proton beams by a circularly polarized laser pulse in the phase-stable acceleration regime, Phys. Rev. Lett. 100 (2008) 135003, http://dx.doi.org/10.1103/PhysRevLett.100.135003.

[8] V.K. Tripathi, C.S. Liu, X. Shao, B. Eliasson, R.Z. Sagdeev, Laser acceleration of monoenergetic protons in a self-organized double layer from thin foil, Plasma Phys. Control. Fusion 51 (2009) 024014, http://dx.doi.org/10.1088/0741-3335/51/2/024014.

[9] A. Henig, S. Steinke, M. Schnürer, T. Sokollik, R. Hörlein, et al., Radiation-pressure acceleration of ion beams driven by circularly polarized laser pulses, Phys. Rev. Lett. 103 (2009) 245003, http://dx.doi.org/10.1103/PhysRevLett.103.245003.

[10] D. Jung, L. Yin, B.J. Albright, D.C. Gautier, R. Hörlein, et al., Monoenergetic ion beam generation by driving ion solitary waves with circularly polarized laser light, Phys. Rev. Lett. 107 (2011) 115002, http://dx.doi.org/10.1103/PhysRevLett.107.115002.

[11] B. Qiao, M. Zepf, M. Borghesi, M. Geissler, Stable GeV ion-beam acceleration from thin foils by circularly polarized laser pulses, Phys. Rev. Lett. 102 (2009) 145002, http://dx.doi.org/10.1103/PhysRevLett.102.145002.

[12] T.-C. Liu, X. Shao, C.-S. Liu, M. He, B. Eliasson, et al., Generation of quasi-monoenergetic protons from thin multi-ion foils by a combination of laser radiation pressure acceleration and shielded Coulomb repulsion, New J. Phys. 15 (2013) 025026, http://dx.doi.org/10.1088/1367-2630/15/2/025026.

[13] B. Eliasson, Ion shock acceleration by large amplitude slow ion acoustic double layers in laser-produced plasmas, Phys. Plasmas 21 (2014) 023111, http://dx.doi.org/10.1063/1.4866240.

[14] Z. Najmudin, C.A.J. Palmer, N.P. Dover, I. Pogorelsky, M. Babzien, et al., Observation of impurity free monoenergetic proton beams from the interaction of a CO_2 laser with a gaseous target, Phys. Plasmas 18 (2011) 056705, http://dx.doi.org/10.1063/1.3562926.

[15] C.A.J. Palmer, N.P. Dover, I. Pogorelsky, M. Babzien, G.I. Dudnikova, et al., Monoenergetic proton beams accelerated by a radiation pressure driven shock, Phys. Rev. Lett. 106 (2011) 014801, http://dx.doi.org/10.1103/PhysRevLett.106.014801.

[16] D. Haberberger, S. Tochitsky, F. Fiuza, C. Gong, R.A. Fonseca, et al., Collisionless shocks in laser-produced plasma generate monoenergetic high-energy proton beams, Nat. Phys. 8 (2012) 95−99, http://dx.doi.org/10.1038/nphys2130.

[17] A.P.L. Robinson, P. Gibbon, M. Zepf, S. Kar, R.G. Evans, et al., Relativistically correct hole-boring and ion acceleration by circularly polarized laser pulses, Plasma Phys. Control. Fusion 51 (2009) 024004, http://dx.doi.org/10.1088/0741-3335/51/2/024004.

[18] A. Macchi, C. Benedetti, Ion acceleration by radiation pressure in thin and thick targets, Nucl. Instrum. Methods Phys. Res. Sect. Accel. Spectrom. Detect. Assoc. Equip. 620 (2010) 41−45, http://dx.doi.org/10.1016/j.nima.2010.01.057.

[19] M.C. Levy, S.C. Wilks, M. Tabak, M.G. Baring, Conservation laws and conversion efficiency in ultraintense laser-overdense plasma interactions, Phys. Plasmas 20 (2013) 103101, http://dx.doi.org/10.1063/1.4821607.

[20] L. Ji, A. Pukhov, B. Shen, Ion acceleration in the 'dragging field' of a light-pressure-driven piston, New J. Phys. 16 (2014) 063047, http://dx.doi.org/10.1088/1367-2630/16/6/063047.

[21] L.L. Yu, H. Xu, W.M. Wang, Z.M. Sheng, B.F. Shen, et al., Generation of tens of GeV quasi-monoenergetic proton beams from a moving double layer formed by ultraintense lasers at intensity 10^{21}−10^{23} W $\cdot$cm^{-2}, New J. Phys. 12 (2010) 045021, http://dx.doi.org/10.1088/1367-2630/12/4/045021.

[22] F.L. Zheng, H.Y. Wang, X.Q. Yan, T. Tajima, M.Y. Yu, et al., Sub-TeV proton beam generation by ultra-intense laser irradiation of foil-and-gas target, Phys. Plasmas 19 (2012) 023111, http://dx.doi.org/10.1063/1.3684658.

[23] M. Passoni, A. Sgattoni, I. Prencipe, L. Fedeli, D. Dellasega, et al., Toward high-energy laser-driven ion beams: nanostructured double-layer targets, Phys. Rev. Accel. Beams 19 (2016) 061301, http://dx.doi.org/10.1103/PhysRevAccelBeams.19.061301.